Feedback Control of a Two DoF Damped Oscillator
AME441 Final Report 2

Bryson Rogers

May 4, 2022

1 System Identification

1.1 Experimental System and Equations of Motion

In this study, various feedback controllers were applied to a two degree of freedom (DoF) damped oscillator system. The experimental system consisted of two masses, two springs, an air damper, and a stepper motor, as shown in Figure 1.

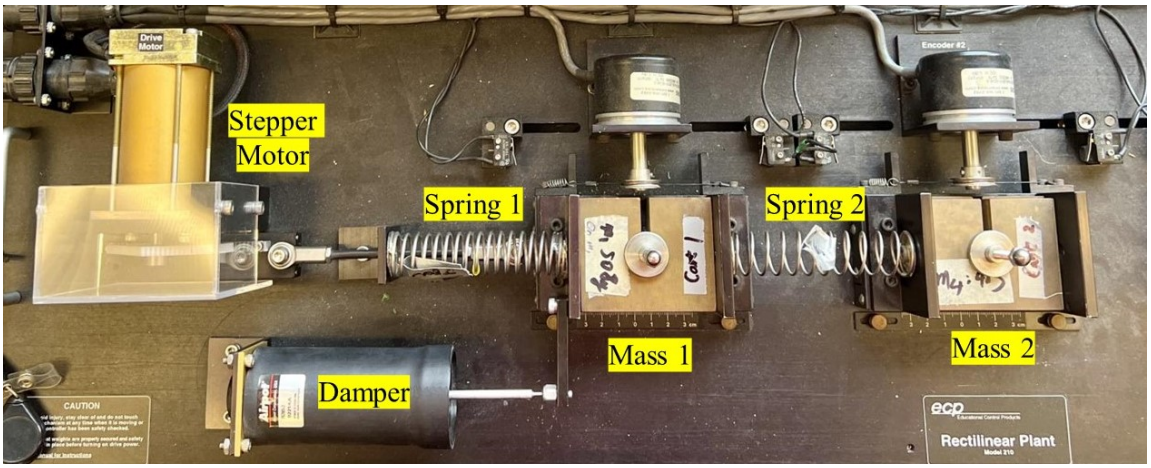

Figure 1: Labeled image of experimental setup.

The masses were secured to two identical carts atop low-friction guide rails that allowed one-dimensional translation. The plunger of an air damper was attached to cart 1 such that the damper resisted the velocity of cart 1. The two springs were attached between cart 1 and cart 2, and between cart 1 and the sliding rack of a rack and pinion. The stationary pinion was rotated by a programmable stepper motor. The voltage input of the stepper motor was user-controlled. The displacement of each mass was measured using an encoder with units of 'counts'.

The experimental system was modelled as linear and 2^{nd}. It was assumed that spring force was linearly proportional to displacement, and that damper force and sliding friction were linearly proportional velocity. Nonlinear stiction present at low velocities was neglected. Applying these assumptions and Newton's Second Law yields the system's equations of motion:

$$m_1\ddot{x}_1 = -k_1x_1 - k_2(x_1 - x_2) - c_1\dot{x}_1 + F(t) \tag{1}$$

$$m_2\ddot{x}_2 = k_2(x_1 - x_2) - c_2\dot{x}_2 \tag{2}$$

where x_1 and x_2 are the displacements of carts 1 and 2, m_1 and m_2 are the total masses of carts 1 and 2, k_1 and k_2 are the spring constants of springs 1 and 2, c_1 is the total damping due to the damper and cart 1 friction, c_2 is the damping due to cart 2 friction, $F(t)$ is force applied by the stepper motor,.

Rearranging equations 1 and 2 and applying the Laplace Transform yields a system of two linked s-domain equations. Solving this system for $X_1/F(s)$ and $X_2/F(s)$ yields:

$$G_{col}(s) = \frac{X_1(s)}{R(s)} = K_{HW}\frac{m_2s^2 + c_3s + k_2}{D(s)} \tag{3}$$

$$G_{ncol}(s) = \frac{X_2(s)}{R(s)} = K_{HW}\frac{c_2 s + k_2}{D(s)} \tag{4}$$

where G_{col} and G_{ncol} are the collocated and noncollocated transfer functions (so named because m_1 is directly acted upon by the stepper motor, whereas m_2 is not), $R(s)$ is the voltage input to the stepper motor, K_{HW} is the tasnfer function that converts motor input voltage to output force (assumed to be a simple gain), and $D(s)$ is the denominator, which is the same for both transfer functions and is a fourth order polynomial of s consisting of the physical parameters m_1, m_2, k_1, k_2, c_1, and c_2.

Most of the physical parameters that define G_{col} and G_{ncol} are difficult to identify using experimental data. For this reason, equivalent expressions for the transfer functions were defined using the system's frequency response. The model predicts that, in response to sinusoidal input, G_{col} has two resonant frequencies (ω_1 and ω_2 and one inverse resonant frequency ω_z). G_{ncol} has the same predicted resonant frequencies, but no predicted inverse resonant frequency. Associated with each of these resonant frequencies is a resonant damping ($\zeta_{1,2,z}$), each of which is associated with the majority of the damping around its corresponding frequency.

Defining G_{col} and G_{ncol} using these model parameters yields Equations 5 and 6, which are equivalent to Equations 3 and 4

$$G_{col} = K'_{HW}\frac{s^2 + 2\zeta_z\omega_z s + \omega_z^2}{(s^2 + 2\zeta_1\omega_1 s + \omega_1^2)(s^2 + 2\zeta_2\omega_2 s + \omega_2^2)} \tag{5}$$

$$G_{ncol} = K'_{HW}\frac{\omega_z^2}{(s^2 + 2\zeta_1\omega_1 s + \omega_1^2)(s^2 + 2\zeta_2\omega_2 s + \omega_2^2)} \tag{6}$$

where K'_{HW} is the model hardware gain, defined to remove all physical parameters from the model parameters transfer functions and calculated as $K'_{HW} = LFG * \omega_1\omega_2\omega_z$, where LFG is "low frequency gain," the gain of the system when subjected to a low frequency ($<$ 0.5Hz) sine input.

To identify $\omega_{1,2,z}$ and $\zeta_{1,2,z}$, the system was subjected to several individual sine inputs with the same amplitude but frequencies that varied from approximately 0.5-10Hz. Each sine input was applied sufficiently long for the system to have achieved a steady state response for at least half of data collection duration. The transient portions of the data were ignored. For more theoretical background on the system's frequency response, see Final Report 1.

The resonant frequencies were determined as the frequencies at which the gain attains its corresponding local maximum (for ω_1 and ω_z) or minimum (for ω_z). The resonant damping values were determined by applying the half power method to each peak (for a description of the half power method, see Final Report 1).

The above analysis yields experiental values for each of the seven model parameters present in the transfer functions described by Equations 5 and 6. The expressions for $G_{col}(s)$ and $G_{ncol}(s)$ do not change whether expressed in terms of model parameters (K'_{HW}, ω, ζ) or physical parameters (K_{HW}, m, c, k), so Equations 3 and 5 can be equated to solve for the missing physical parameters. Matching the corresponding terms in the two expressions for G_{col} yields a system of equations.

1.2 1 Dof System ID

The aforementioned system of equations is underdefined. To fully define the system, K_{HW}, m_1, and c_1 were identified using 1 DoF step response data. 2V step responses were executed with m_1

$\boldsymbol{\omega_1}$	12.57
$\boldsymbol{\omega_2}$	28.27
$\boldsymbol{\omega_z}$	16.96
$\boldsymbol{\zeta_1}$	0.029
$\boldsymbol{\zeta_2}$	0.027
$\boldsymbol{\zeta_z}$	0.069
$\boldsymbol{K_{HW}'}$	7.20E3

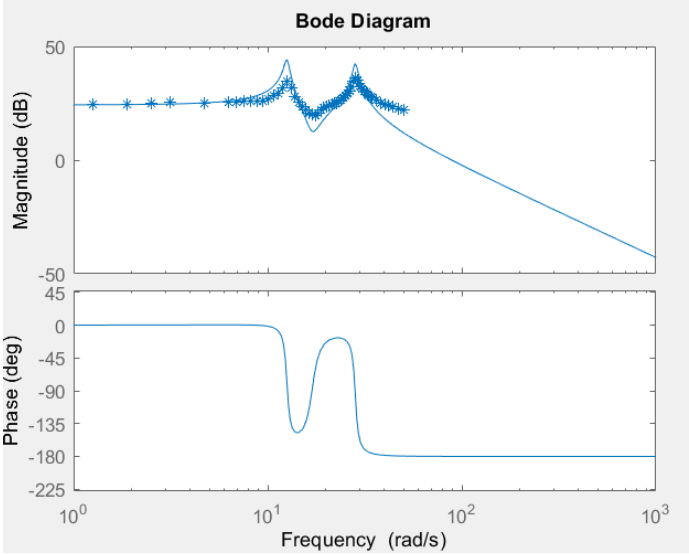

Figure 2: Individual sine data and Gcol Bode

free and m_2 held stationary and with varying mass on m_1. Using this 1 DoF step data, K_{HW} was identified according to Equation 7

$$K_{HW} = k_1 * x_{ss}/V_{step} \tag{7}$$

where x_{ss} is the steady state displacement of m_1 and V_{in} is the step input voltage. The natural frequency ω_n and damping ζ were determined for the step response with each mass using the exponential curve fitting method (ECFM) then used to calculate experimental values for m_1 and c_1. For further information on ECFM and how to calculate m_1 and c_1 using ω_n and ζ, see Final Report 1.

With experimental values for K_{HW}, m_1, and c_1, the above system of equations is fully defined. The remaining physical parameters were solved for, and the experimental values for all parameters are presented in the Table below.

The experimental individual sine data and analytical bode plots are provided below.

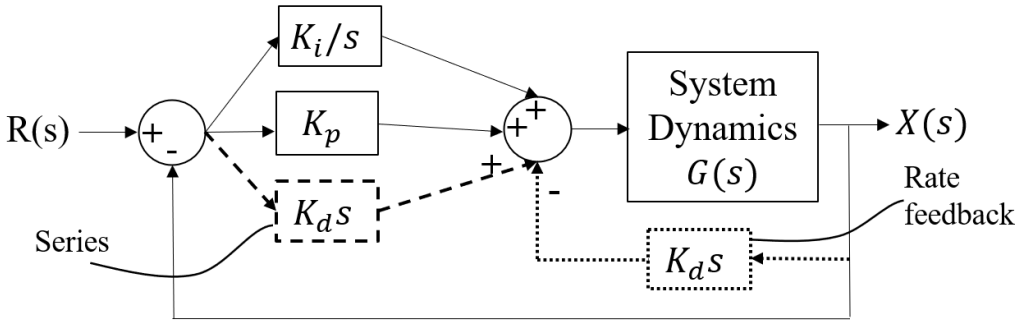

Figure 3: Generic PID control block diagram showing the series and rate feedback configurations

1.3 System ID: Conclusion

The most notable difference between the 1 DoF and 2 DoF responses is the existence of more than one resonant peak and multiple modes of vibration. The 1 DoF frequency response had a single resonant frequency, whereas the 2 DoF and two resonant frequencies and one inverse resonance. Additionally, depending on the excitation frequency, m_1 and m_2 may oscillate in or out of phase with each other (in phase near ω_1 and nearly 180° out of phase near ω_2). The presence of two masses makes the response of both m_1 and m_2 generally less 'smooth' than the 1 DoF response due to the presence of multiple vibration modes simultaneously.

2 Feedback Control

In the previous section, model parameters were derived using open loop frequency response data to obtain experimental expressions for the collocated and noncollocated transfer functions G_{col} and G_{ncol}. These transfer functions decribe the relationship between the voltage input to the stepper motor and the mass displacements $X_1(s)$ and $X_2(s)$. In this section, the design and implementation of several closed loop feedback controllers is discussed.

These controllers fall into four categories, each of which is discussed in further detail below: collocated, noncollocated, mixed, and notch filter. Each control type (except notch filter) may be further classified as 'series' or 'rate feedback' depending on the placement of its differential block $K_d s$ in its control architecture. Figure 3 shows a generic PID controller series configuration and rate feedback configuration.

Series architecture tends to be slightly more stable, whereas rate feedback architecture yields mathematically simpler transfer functions. For further discussion of the differences between series and rate feedback architecture, see Final Report 1.

The design criteria used to evaluate each controller were peak overshoot M_p, settling time t_s, control effort, steady state error e_{ss}, and stability. Stability is the most important because an unstable response may diverge or be unimplementable, and may at worst cause damage to the system. The other three criteria were chosen because they are three of the most important quantities by which real life systems are typically judged.

Feedback controlled two DoF systems are far more mathematically conplex than 1 DoF systems, and it is thus very difficult to design K_p, K_d, and K_i via analytical methods. In this study, all

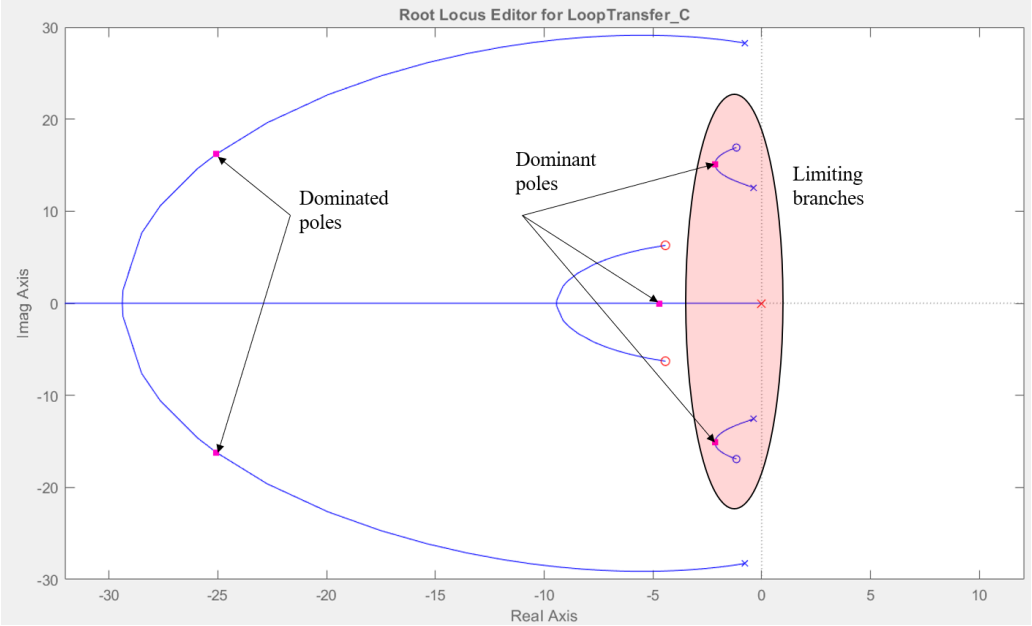

Figure 4: Root locus of a generic PID controlled system as shown in SISOtool. System behavior may be modified by changing K_p, K_d, and K_i.

controllers were designed using the SISOtool functionality in MATLAB, which allows the user to see the affects of the controller gains on the controlled system's root locus diagram. The SISOtool root locus diagram of a generic PID controlled system is shown in Figure 4.

2.1 Collocated Controllers

Collocated controllers manipulate the voltage input to the motor depending on the position X_1 of m_1. They are referred to as collocated because the motor exerts force on m_1 almost directly (with spring 1 being the only separation). The block diagram of a collocated control system is shown in Figure 5.

2.1.1 Collocated: PD

Collocated PD and PID controllers in series and rate feedback configuration were designed and implemented. The mathematically simpler rate feedback configuration was implemented first. The first collocated rate feedback PD controller was designed to have low control effort, whereas the second was designed to be a compromise between control effort, M_p, and e_{ss}. The root locus plots of both controllers are provided in Figure 14 (to keep the body of the report readable, all root locus plots used for controller design are provided in Section 4 at the end of the report). The first controller had lower k_p and k_d to decrease control effort, and as a result had greater e_{ss} and M_p. Both controllers were stable and had similar t_s. The experimental and simulated responses of the compromising controller are presented in Figure 6a.

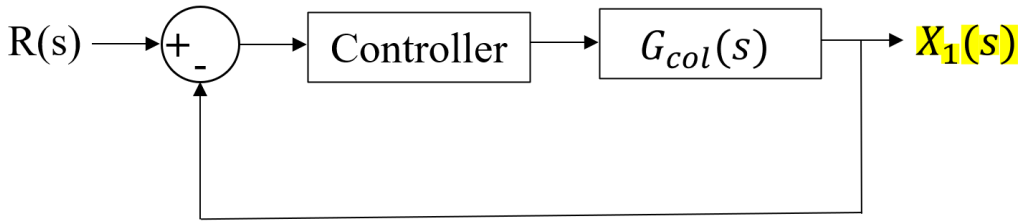

Figure 5: Block diagram of a generic collocated controller system. The system response is controlled based on the error between X_1 and the commanded position of m_1.

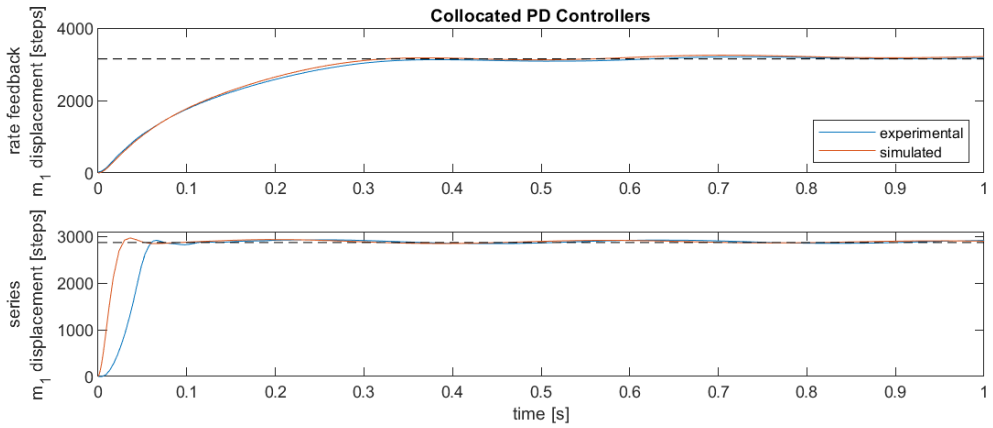

Figure 6: Comparison of step responses of collocated PD controllers in rate feedback and series configurations. Experimental and simulated data provided.

Following the design of the rate feedback controllers, two collocated series PD controllers were designed. It was not expected that these controllers would be preferable, because the primary advantage of the series configuration is increased stability, but the collocated rate feedback PD controllers had no issues with stability. The first of the collocated series PD controllers was designed to minimize M_p, and the second was designed to compromise between the design criteria. The root locus plots of both designs is shown in Figure 15.

The experimental and simulated step responses of the (a) rate feedback and (b) series PD controllers are presented in Figure 6. The series control has a much lower t_s than the rate feedback control. This is in part because the series controller is more stable, and thus more aggressive control effort and system acceleration may be achieved without losing stability.

2.1.2 Collocated: PID

The addition of an integrator to a PD control allows for more intricate control of the system and eliminates steady state error, but decreases the stability of the system. As with the collocated PD controllers above, collocated PID controllers were designed in both rate feedback and series configurations. In each case, k_d was first selected to maximize the stability of the controller, because

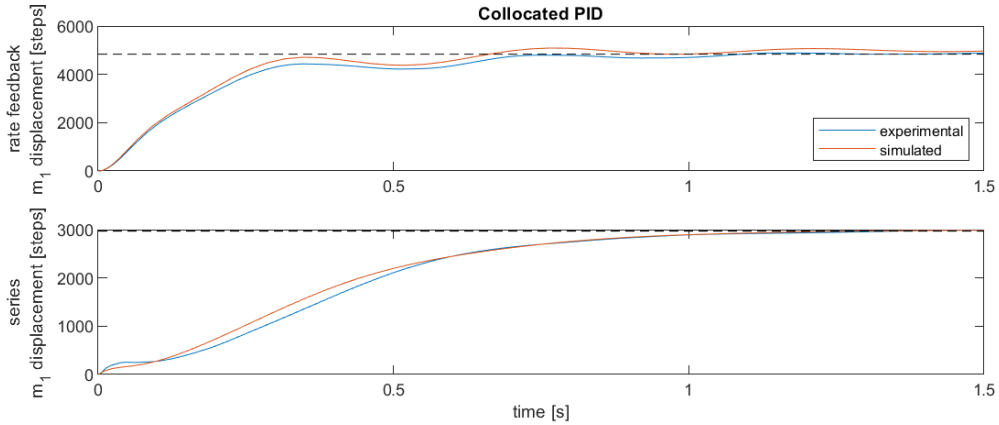

Figure 7: Comparison of step responses of collocated PID controllers in rate feedback and series configurations. Experimental and simulated data provided.

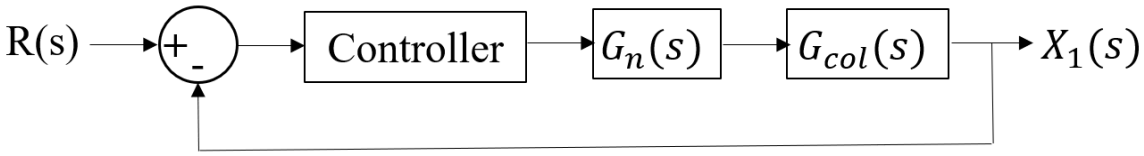

Figure 8: Block diagram of a generic closed loop system with a notch filter $G_n(s)$. The controller may be a P, PD, or PID controller.

PID controllers have a greater tendency to become unstable than PD controllers. After selecting k_d, k_p and k_i were selected to optimize for the desired design criteria while maintaining stability. The root locus plots of the rate feedback and series collocated PID controllers are presented in Figures 16 and 17, respectively.

The experimental and simulated step responses of the (a) rate feedback and (b) series PID controllers are presented in Figure 7. The series control has a slightly more gradual increase. However, the two controls did not differ greatly in their performance or ease of design while avoiding instability. Compared to the PD controls, the PID controls had a greater tendency to be unstable and higher control effort, but no e_{ss}.

2.1.3 Collocated: Notch Filter

PD and PID are inherently reactive; they exert control effort in responde to some error after it arises. A notch filter augments a controller by preventing error before it arises. It does so by implementing a transfer function in series with the system transfer function that 'cancels out' one or more of the system's resonant frequencies. A generic notch filter block diagram is provided in Figure 8, where $G_n(s)$ is the notch filter transfer function.

The notch filter was designed with the intent of cancelling out the first resonant peak ω_1 of the system response. To accomplish this, $G_n(s)$ was defined as having a the ω_1 pole in its numerator as follows:

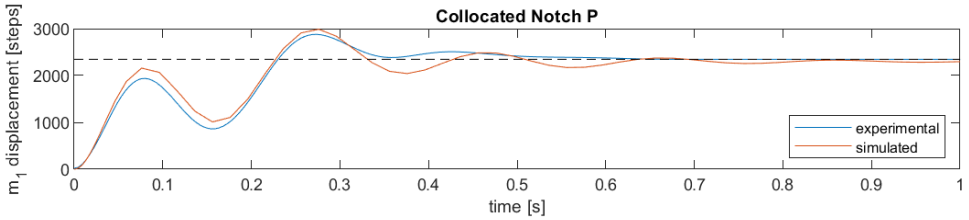

Figure 9: Comparison of experimental and simulated step responses using collocated notch P control.

$$G_n(s) = \frac{s^2 + 2\zeta_2\omega_1 s + \omega_1^2}{(1 + 1/\zeta_z)^2} \tag{8}$$

P and PID controls were designed for the collocated notch filter system. The root locus diagrams of these controllers are presented in Figure 18.

The P controller was very stable, and could be implemented without any problems. It yielded a system with high e_{ss},low M_p, and low control effort. The experimental and simulated step responses of the collocated P notch control are provided in Figure 9. The collocated PID notch control had a very small design space, as shown by the limiting branches very close to the imaginary axis in Figure 18b. A theoretically stable PID notch controller was designed in SISOtool, but it was unstable when implemented. This discrepency in stability between the designed and actual controllers is likely due to 'phantom poles' - poles that exist in real life but are neglected by the model due to the assumptions made and nonidealities of the real system.

2.1.4 Collocated: Conclusion

The optimal selection of a PD or PID control, and whether a notch filter is used, depends on the design objectives of the particular system being controlled. If stability is the most important objective, a PD control with no notch filter would suffice. If a system needs to have no e_{ss} or lower t_s, and it has low risk of instability and can afford to exert greater control effort, then a PID with no notch would be best. If in either of these cases it is desired to alter the behavior of the system around a particular resonant frequency, adn the system is not on the verge of instability already, then it would be best to implement a notch filter to the PD or PID controller.

2.2 Noncollocated

A noncollocated controller exerts control effort on the system based on the displacement of m_2, which is less directly connected to the stepper motor than m_1. Between m_2 and the stepper motor lie spring 1, mass 1, and spring 2. This indirectness causes a delay between between the exertion of control effort on the stepper motor and the effects of that control effort on X_2. For this reason, noncollocated controls tend to be less stable and have worse performance in general. The block diagram of a generic noncollocated control system if shown in Figure 8.

Three noncollocated controls were designed: series PD, series PID, and P with a notch filter. The root locus plots of each of these three designs are provided in Figure 19. None of these three controls were implementable due to instability. The potential instability of these controls is evident

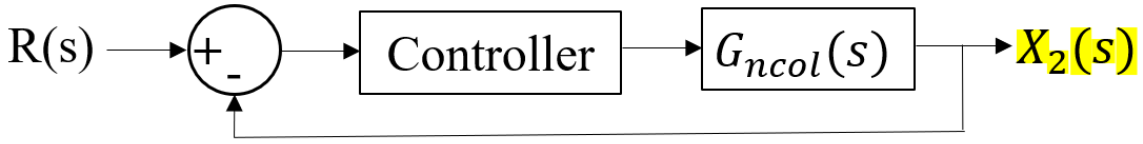

Figure 10: Block diagram of a generic noncollocated control system. The controller may be a P, PD, or PID controller.

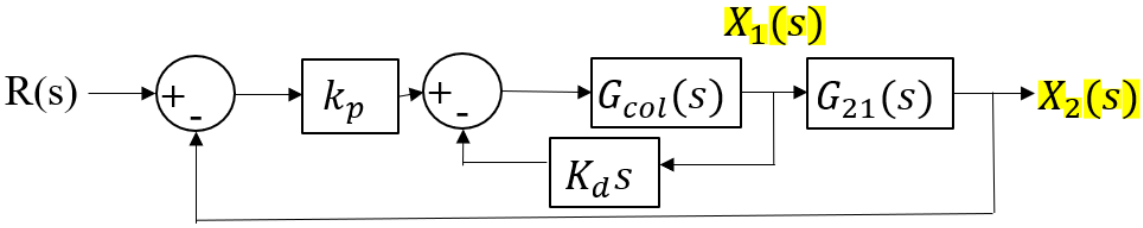

Figure 11: Block diagram of a mixed rate feedback PD control system.

in the very small design spaces in Figure 19; each of the limiting branch poles is very close to the imaginary axis. A SISOtool-generated simulation of the step response of the noncollocated series PD controller is provided in Figure 12. This simulated response has large M_p, t_s, and e_{ss}, and became unstable when implemented.

3 Mixed Controls

A mixed control exerts control effort on the motor as a function of both X_1 and X_2. The potential benefit of a mixed control system is that, if the system model is highly accurate, it may provide more stable and responsive control of the system by taking into consideration more information. One drawback of the mixed control system is that, because it has two outputs, k_d and k_p must be designed iteratively if using SISItool (which only accepts a Single Output, Single Input). The block diagram of a mixed rate feedback PD control is presented in Figure 11

Two mixed controls were designed: rate feedback PD and PID. The PD control was also implemented, whereas the PID was not. The root locus diagrams of both control designs are presented in Figure 20.

The experimental and simulated responses of the mixed rate reedback PD control are presented in Figure 13. The mixed PID was not implemented.

4 Conclusion

This study explored the strengths and weaknesses of various control types: collocated, noncollocated, and notch; P, PD, and PID architecture with rate feedback and series configurations; and notch filters. There is no single ideal controller type; optimal controller selection depends on the dynamic system being controlled.

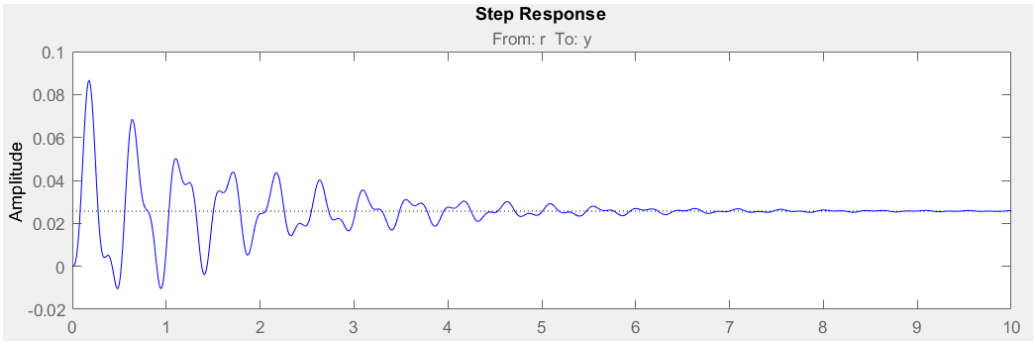

Figure 12: Simulated step response of the noncollocated series PD control.

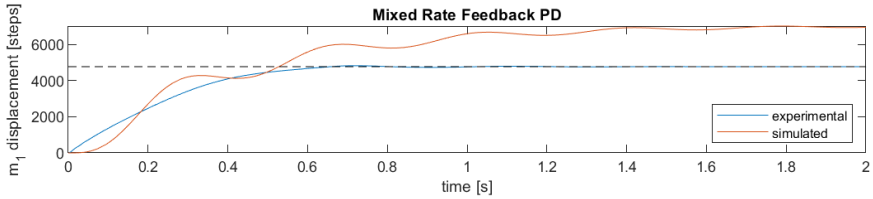

Figure 13: Experimental and simulated responses of the mixed rate reedback PD control.

In general, collocated controls were preferable to noncollocated and mixed controls in this study. The instability of the noncollocated controls make them a poort choice for this dynamic system. The mixed controls performed better than the noncollocated controls, but they also had a small design region and greater tendency to be unstable than the collocated controls. Additionally, the mixed controls were more laborious to design than the collocated controls (using SISOtool) due to the necessity of designing the inner (k_d) and outer (K_p, K_i) loops separately.

Neither PD nor PID controls were 'better' overall. PD controls are ideal if e_{ss} is not an issue and a highly stable system is desired. PID controls allow more intricate control of the system response, and are ideal if the system has a large stable design region and minimal e_{ss} or t_s are required.

The choice of rate feedback or series architecture did not hugely affect system performance. In general rate feedback systems are simpler to design, but series systems lend slightly higher stability.

Notch filters can be useful if a particular resonant peak is undesired in system response. However, they tend to decrease stability, and can exacerbate the effects of 'phantom poles' if the system model is not highly accurate. Due to the potential instability issues, notch filters are best incorporated into collocated controls with P or PD feedback.

5 Root Locus Plots

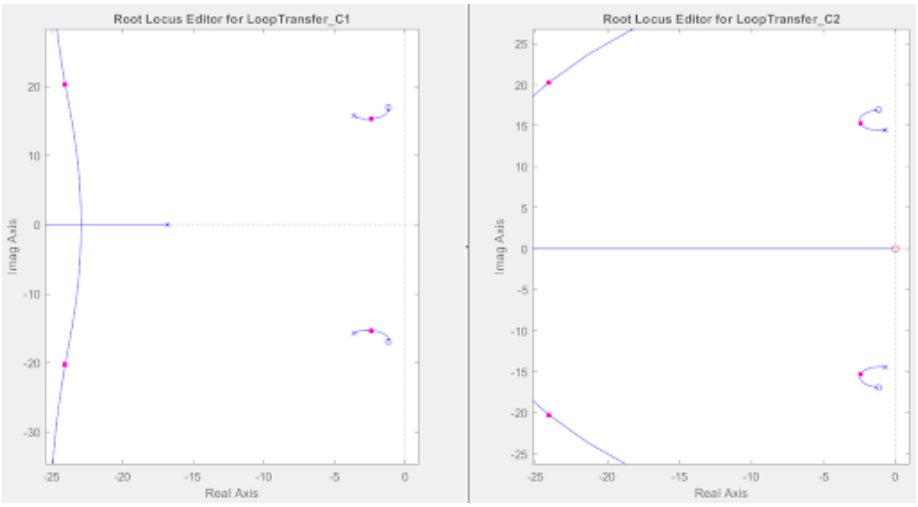

(a) Control effort minimized

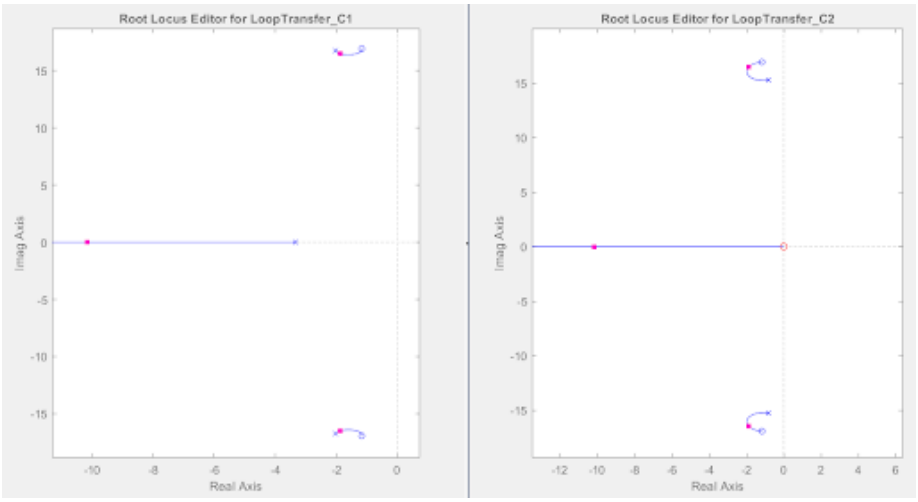

(b) Compromise of design criteria

Figure 14: Root locus plots of two collocated rate feedback PD controls optimized for different design criteria.

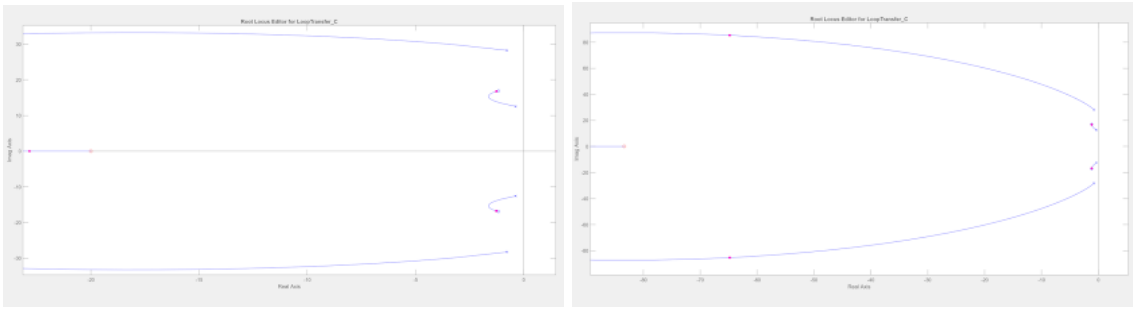

(a) Peak overshoot minimized

(b) Compromise of design criteria

Figure 15: Root locus plots of two collocated series feedback PD controls optimized for different design criteria.

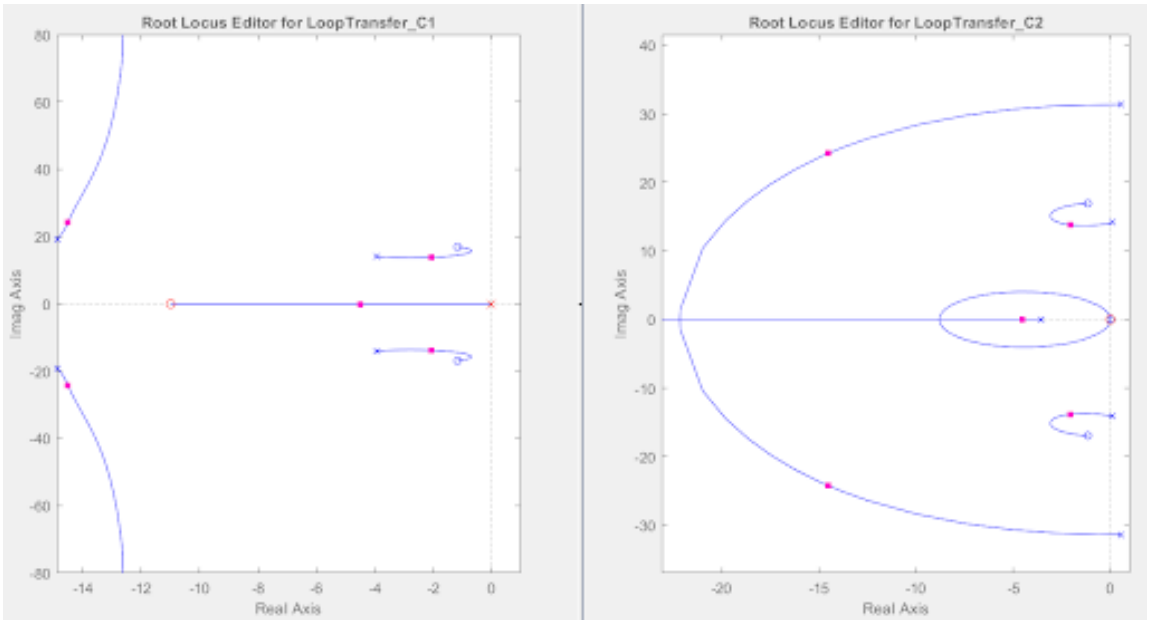

(a) Control effort minimized

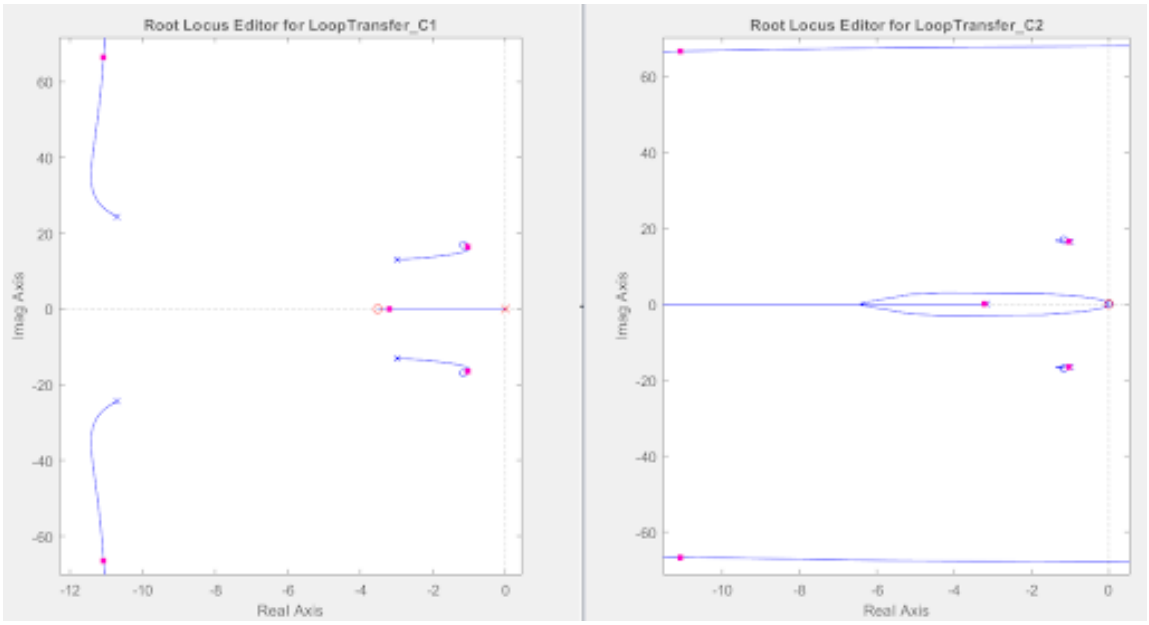

(b) Compromise of design criteria

Figure 16: Root locus plots of two collocated rate feedback PID controls optimized for different design criteria.

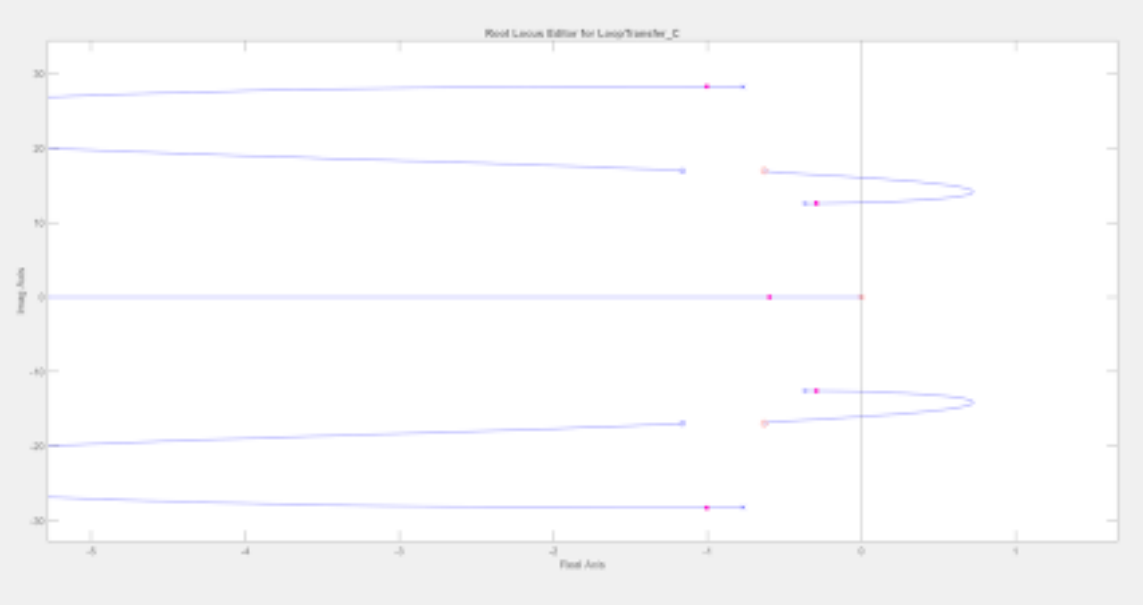

(a) Peak overshoot minimized

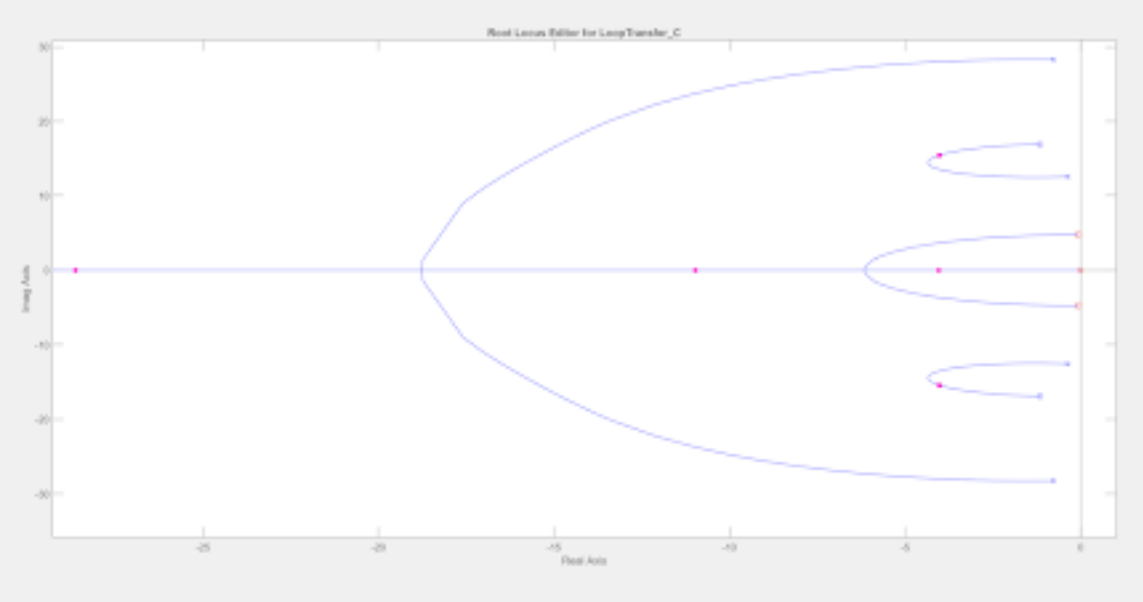

(b) Compromise of design criteria

Figure 17: Root locus plots of two collocated series PID controls optimized for different design criteria.

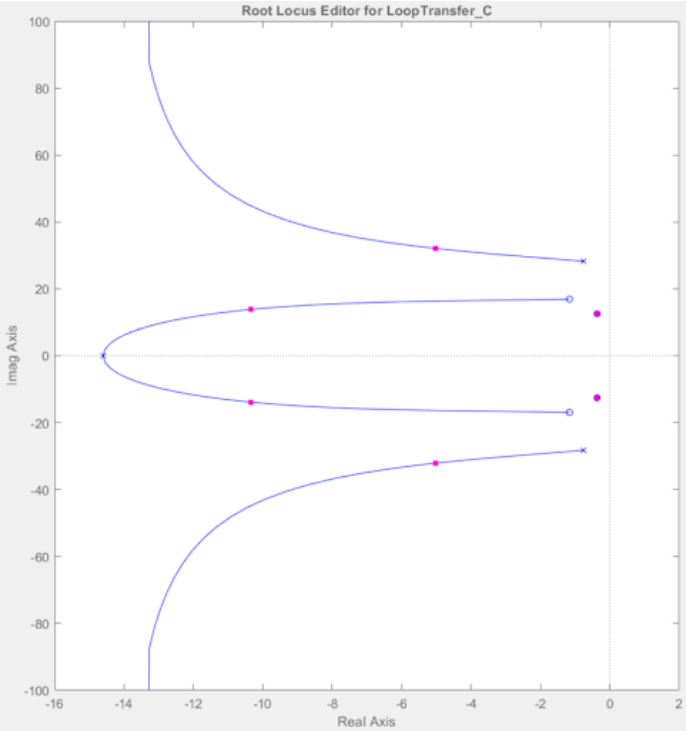

(a) P controller

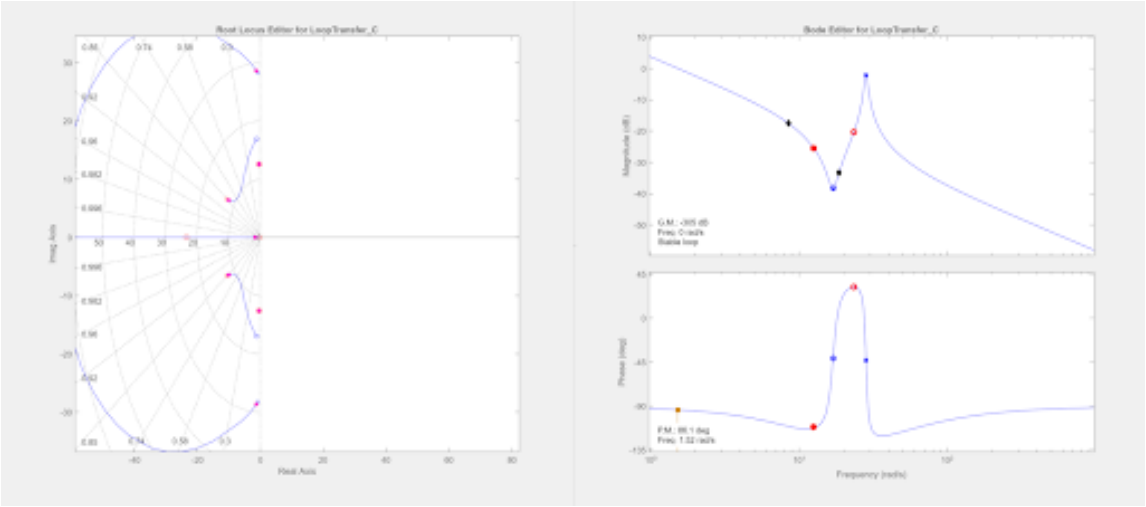

(b) PID controller

Figure 18: Design of collocated P and PID notch filter controllers. The Bode plot of the PID design is provided.

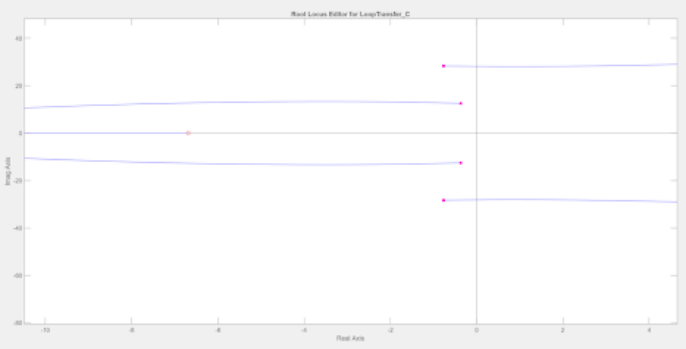

(a) PD controller

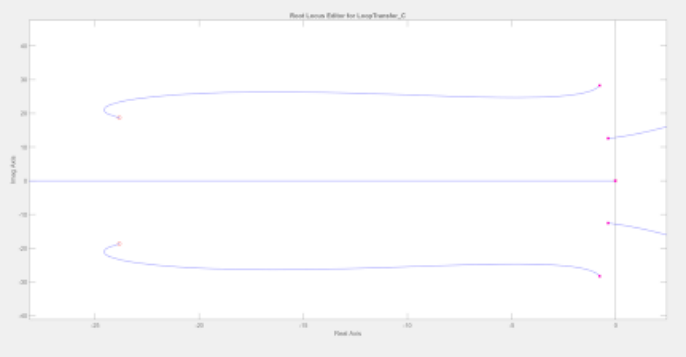

(b) PID controller

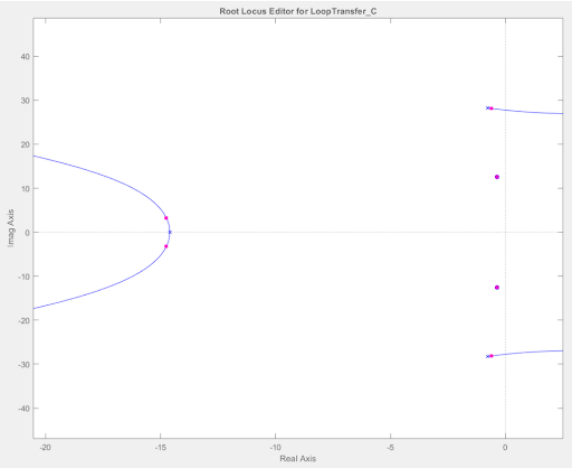

(c) P controller with notch filter

Figure 19: Root locus design of noncollocated controls. Each has a notably small design region, which is indicative of a potentially unstable system.

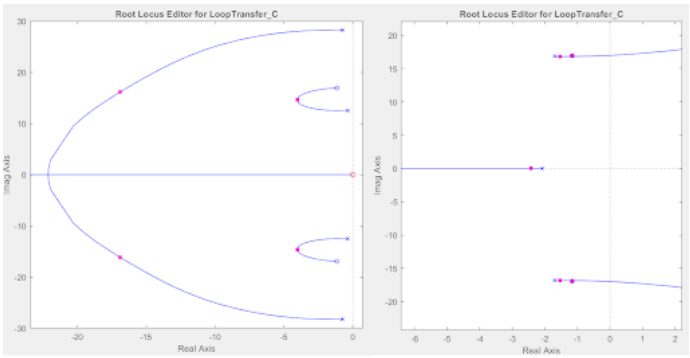

(a) PD controller

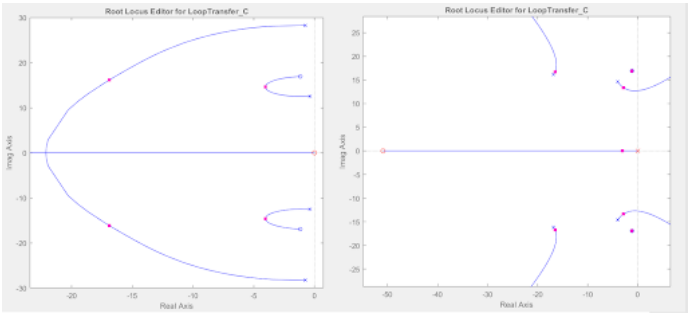

(b) PID controller

Figure 20: Root locus design of mixed feedback controls.